32×32 very long wave infrared HgCdTe FPAs

Hao Lichao[1,2], Huang Aibo[2], Xie Xiaohui[2], Li Hui[2], Lai Canxiong[1], Chen Honglei[2], Wei Yanfeng[2], Ding Ruijun[2]

(1. Laboratory of Science and Technology on Reliability Physics and Application of Electronic Component, The Fifth Research Institute of Ministry of Industry and Information Technology, Guangzhou 510610, China;
2. Key Laboratory of Infrared Imaging Materials and Detectors, Shanghai Institute of Technical Physics, Chinese Academy of Sciences, Shanghai 200083, China)

Abstract: Very long wave infrared (VLWIR) band is widely used for the remote atmosphere sounding applications, particularly for humidity, CO_2 levels, cloud structure and temperature distribution. A 32×32 VLWIR HgCdTe focal plane array (FPA) was designed. The photosensitive component was fabricated by B+ ion implanting As-doped p-type material of liquid phase epitaxial growth on ZnCdTe substrate. The readout integrated circuit (ROIC) used a buffered direct injection (BDI) structure with an improved background suppression. The VLWIR focal plane array (FPA) was achieved by combining the HgCdTe detector with ROIC in terms of indium bump bonds, the cutoff wavelength of which was over 14 μm. The pixel occupied an area of 60 μm×60 μm. It could be operated at the temperatures of 50 K. The test results show that the peak detectivity and blackbody responsivity of PFAs are 2.57×10^{10} cmHz$^{1/2}$/W and 1.35×10^{7} V/W, respectively. The nonuniformity of responsivity is about 45%, and dead pixels ratio is less than 12%.

Key words: HgCdTe; VLW; IRFPA; ROIC; background suppression
CLC number: TN215 **Document code:** A **DOI:** 10.3788/IRLA201746.0504001

32×32 甚长波红外 HgCdTe 焦平面器件

郝立超[1,2],黄爱波[2],解晓辉[2],李 辉[2],赖灿雄[1],陈洪雷[2],魏彦锋[2],丁瑞军[2]

(1. 工业和信息化部电子第五研究所 电子元器件可靠性物理及其应用技术重点实验室,广东 广州 510610; 2. 中国科学院上海技术物理研究所 红外材料与器件重点实验室,上海 200083)

摘 要: 甚长波红外波段富含大气湿度、CO_2 含量及云层结构和温度轮廓等大量信息,是大气遥感的重要组成部分。设计了一种 32×32 甚长波红外焦平面阵列,采用在 ZnCdTe 衬底上液相外延生长的 As掺杂 p 型材料上进行 B+离子注入形成光敏元,通过铟柱倒焊技术和带有改进型背景抑制结构的读出电路互联,制成截止波长达到 14 μm 的焦平面器件。该红外焦平面器件像元面积为 60 μm×60 μm,工作温度在 50 K 温度下。测试结果显示:读出电路性能良好,焦平面黑体响应率达到 1.35×10^{7} V/W,峰值探测率为 2.57×10^{10} cmHz$^{1/2}$/W,响应率非均匀性约为 45%,盲元率小于 12%。

关键词: 碲镉汞; 甚长波; 红外焦平面; 读出电路; 背景抑制

收稿日期:2016-09-05; **修订日期**:2016-10-12

基金项目:重点实验室基金(9140C1030302150C03011);广州市珠江科技新星专项(2014J2200086);国家自然科学基金(61204116)

作者简介:郝立超(1986-),男,博士,主要从事读出电路设计及其焦平面可靠性方面的研究。Email:hao_li_chao@163.com

通讯作者:黄爱波(1984-),男,工程师,主要从事红外焦平面设计、测试及筛选等方面的研究。Email:hab-888@163.com

0 Introduction

The infrared focal plane array (IRFPA) technology has been applied in various areas, e.g. safety, space sciences, environmental management, process monitoring. In recent years, the very long wave infrared (VLWIR)(12-18 μm) FPAs have become the core of intense research and technological developments [1]. Because the VLWIR band can provide rich information on humidity, CO_2 levels, cloud structure and the temperature distribution, the VLWIR FPAs have been widely used in the remote atmosphere sounding applications. Furthermore, VLWIR information is used as an entry parameter for analyzing other spectral bands[2], and it′s thought to be great important.

It is widely known that the gap of HgCdTe detector bands for VLWIR FPAs is very small, and its content of Hg is in a high level. So a slight parameter fluctuation will lead to great changes in response band. In order to get high quality detectors, critical control is needed in growth of HgCdTe materials. Furthermore, the HgCdTe material has a weak Hg-Te bond, which leads to bulk, surface and interface instabilities. Uniformity and yield are still significant issues in the VLWIR spectral range. As the detector band gap decreases, or the cutoff wavelength increases, dark current becomes larger. Therefore, every step of the device fabrication is important[3].

The VLWIR detectors have very low output impedance[4]. In order to achieve high injection efficiency and a low input resistance, we need a high gain amplifier to provide precise biasing voltage for the detectors in buffered direct injection (BDI) input circuit. Furthermore, the VLWIR detectors run at high background environment with a large dark current, so the integration capacitor is easily saturated. It′s hard to get an ideal signal-to-noise ratio (SNR) [5]. The performance of VLWIR FPAs is largely limited by the defects of VLWIR detectors, and there′s also a high request for readout integrated circuit (ROIC) design.

In this experiment, the photosensitive component is fabricated by B+ ion implanting As-doped p-type material of liquid phase epitaxial growth on ZnCdTe substrate. The VLWIR FPAs is achieved by a combination the HgCdTe detector and ROIC in terms of indium bump bonds, and its cutoff wavelength is more than 14 μm. The current-voltage (I-V) and resistance-voltage (R-V) curves are tested, and the typical spectral response curve is measured. The details of the FPAs are also evaluated and analyzed.

1 Fabrication and structure of VLWIR FPA

1.1 Fabrication of VLWIR detector

HgCdTe material is grown by liquid phase epitaxy on lattice matched CdZnTe substrates. As Fig.1 shows, the VLWIR detector is fabricated by B+ ion implanting As-doped p-type material of liquid phase epitaxial growth on ZnCdTe substrate. The insulting layers are the CdTe and ZnS prepared by electron-beam evaporation, and Au is grown on cutouts of insulting layers as metal electrode. Then the indium bump is fabricated on the Au metal electrode.

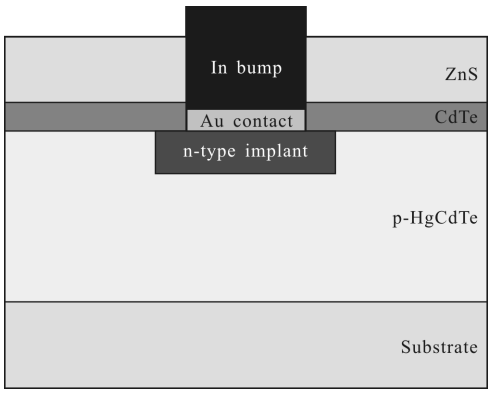

Fig.1 Structure of VLWIR FPAs

1.2 Structure of ROIC

The ROIC is mainly consisted of unit cell module, scanning multiplexer and output video amplifiers. The unit cell of the ROIC is used for signal identifying and filtering, integration and amplifying, sampling and holding. Then the voltage

signal will put out through output video amplifiers, which are controlled by the scanning multiplexer.

Figure 2 shows the analog circuit link structure of the ROIC. It includes the BDI input circuit (that uses high gain feedback amplifier), improved background suppression, sample and hold circuit, and two stage source followers as output circuit. The unit cell is marked by dotted frame.

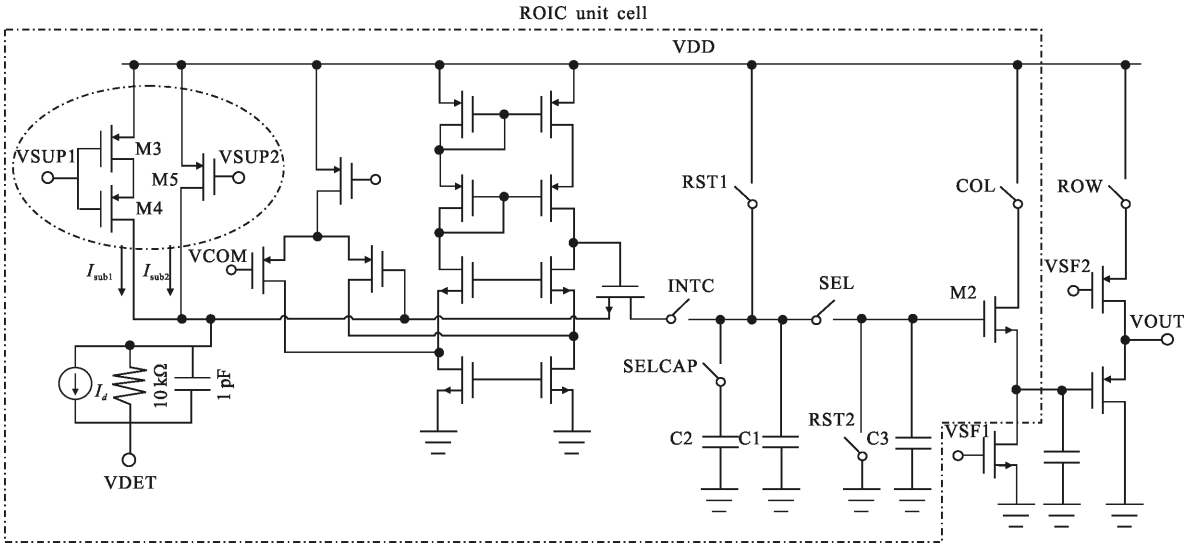

Fig.2 Analog circuit link structure of ROIC

In order to overcome the defects of VLWIR detectors, the BDI structure is used for VLWIR FPAs to provide high injection efficiency and low input resistance and to provide precise biasing voltage to the photodiode[6], although it has some limitations in terms of power, area etc. For VLWIR detectors having very low output impedance, a high gain amplifier over 80 dB must be used[7]. By means of the virtual earth in BDI, the detector will be at precise zero-bias voltage. In order to get high gain and high overall voltage swing, a folded-cascode op amp is selected to prevent the leakage current from being too large. At the same time, large size PMOS transistors are instituted as input stage of the amp to reduce the offset and improve the noise performance. The gain A_V can be more than 85 dB, when the phase margin is equal to 60°. The out swing is in the range from 0.2 V to 2.4 V.

To eliminate the background current, the improved background suppression is used for each unit cell, and the detailed structure is shown in dotted circle frame of Fig.2. First of all, a rough current is produced by controlling M5. Secondly, the self-cascode transistors M4 and M5 are designed in long channel, and works in their strong inversion mode to generate the accurate subtracted current. Because the self-cascode structure has high output impedance[8], it can effectively reduce the background suppression uniformity and increase the generated current linearity. In addition, the fixed pattern noise (FPN) and $1/f$ nose are also decreased by using lager size PMOS for M3, M4 and M5. By means of improved background suppression, the integration time and the signal-to-noise ratio (SNR) of image data is increased to 21 μs and 78.3 dB when VLWIR FPAs run at high background environment. Therefore, better contrast and dynamic range of the output images can also be achieved.

To accommodate the wide scene dynamic range of the atmospheric sounding instrument, two selectable integration capacitors C1 and C2 are used in the ROIC for different input current levels from 0.1–10 μA. At the same time, a sample and hold circuit controlled by the switch of SEL is contained by each readout unit

cell to make the ROIC working in two modes such as integrate-then-readout(ITR) and integrate-while-readout (IWR). The timing patterns for IWR is shown in Fig.3.

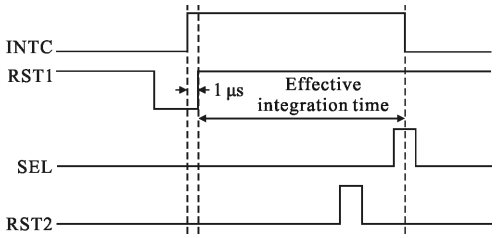

Fig.3 Timing of IWR

The source followers have relatively simple structure, very low power and approximately gain of one. Besides they also exhibit high input impedance and moderate output impedance [9]. In addition, its reliability at the temperature of 50 K is perfect, so the output video amplifiers are selected with two stage source followers.

1.3 Measurement packaging of VLWIR FPA

The FPA adopts hybrid flip chip bonding interconnection technology as Fig.4 shown. Indium bumps are grown on cutouts of ROIC after 15 min ion back sputtering in order to remove oxide metal of cutouts′ surface. Due to the low impedance of VLWIR detectors, growth of Ti/Pt/Au is selected as metal electrode of ROIC to reduce the contacting resistance.

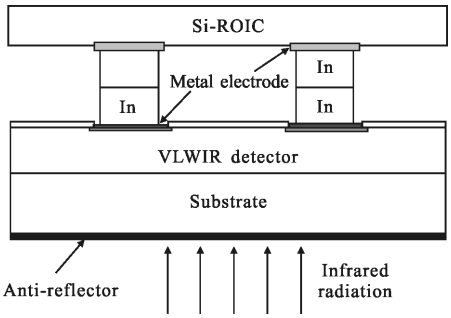

Fig.4 Structure of hybrid flip chip bonding interconnection

After VLWIR FPA has been realized by combing the HgCdTe detector with ROIC in terms of indium bump bonds, the measurement pattern is packaged into Stirling refrigerator and fixed with refrigerator′s cold head. Figure 5 shows the Stirling refrigerator with VLWIR FPA on its cold head. Then the temperature of cold head is controlled by computer to adjust the FPA′s working temperature. Thereby the low-temperature and variable-temperature test will be carried out to evaluate the performance of VLWIR FPA.

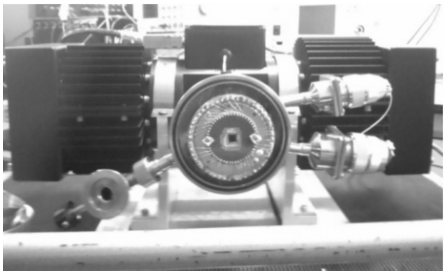

Fig.5 Stirling refrigerator with VLWIR FPA

2 Results of VLWIR FPA

The VLWIR FPA can work in two modes for full frame snapshot mode and rolling mode. The snapshot with the function of ITR provides the maximum integration time available. Another potential benefit of the snapshot is that the integration process is separated from the readout process, thus making it almost impossible for the signals being read out to corrupt the signals being integrated [10]. On the other hand, the rolling mode with the function of IWR can provide the maximum readout speed. As a result of the integration process occurring during the readout process, the frame time can be approximately equal to the readout time.

First, the parameter of VLWIR HgCdTe detector was measured. A Keithley 236 parameter analyzer is used in $I-V$ measurements, and a Fourier transform infrared spectrometer is used in the quantum efficiency versus wavelength. Then the whole performance of VLWIR FPA was evaluated at the temperature of 50 K.

Figure 6 shows spectral response per photon versus photon wavelength of the VLWIR HgCdTe detector. Since 50% of the peak relative response is cutoff wavelength, so the cutoff wavelength of the VLWIR HgCdTe detector can achieve 14.3 μm at 50 K.

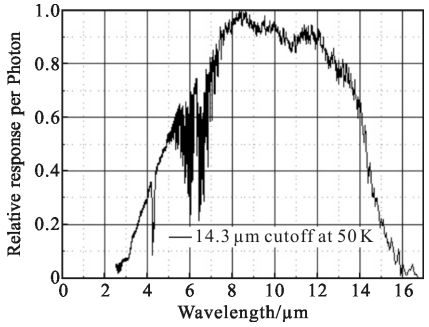

Fig.6 Relative response per photon versus photon wavelength

Figure 7 shows the current-voltage ($I-V$) and the resistance-voltage ($R-V$) curve of dark-field at temperature of 50 K. Due to large tunneling current, the dark current of the device is quite great in dark-field under reverse bias. From the curve, it′s obvious that the impedance of the VLWIR detector is less than 1 K. Because of the extremely low impedance, VLWIR detector need a high performance ROIC to have a better operation.

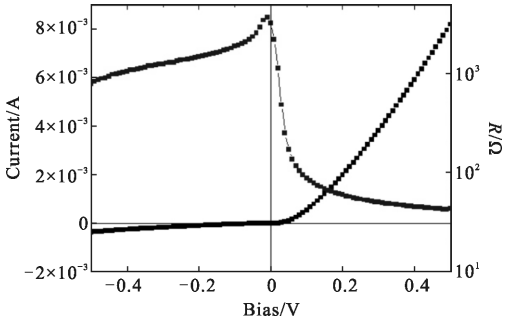

Fig.7 $I-V$ and $R-V$ curve of VLWIR detector at 50 K

The VLWIR FPA was tested in rolling mode at 50 K. The blackbody temperature for test is from 20 ℃ to 35 ℃. The integration time is 21 μs, and the subtracted background current is about 0.5 μA. The responsivity and output delta of one column is shown in Fig.8. The whole characteristics of VLWIR FPA are listed in Tab.1.

Table 1 shows that the peak detectivity and blackbody responsivity are respectively 2.57×10^{10} cm·Hz$^{1/2}$/W and 1.35×10^{7} V/W in typical readout clock frequency at the temperature of 50 K. The output swing is more than 2.0 V, the maximum readout clock frequency is 2.5 MHz, and the total power dissipation is less than 120 mW. But the nonuniformity of responsivity and dead pixels ratio are too more than other infrared bands′ level.

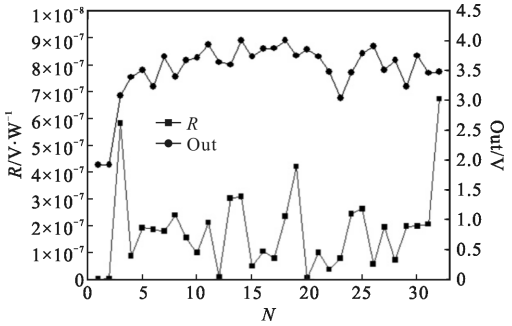

Fig.8 Responsivity and output delta of VLWIR FPA

Tab.1 Summary of the VLWIR FPA characteristics at 50K

Parameters	Performance
Array size	32×32
Pixel pitch/μm×μm	60×60
Output swing/V	>2.0
Peak detectivity/cm·Hz$^{1/2}$·W^{-1}	2.57×10^{10}
Blackbody responsivity/V·W^{-1}	1.35×10^{7}
Nonuniformity of responsivity	45%
RMS(noise)/mV	0.9
Dead pixels ratio	12%
Power dissipation/mV	<120
Operating temperatures/K	50
Max. clock frequency/MHz	2.5
Typical clock frequency/MHz	1

Due to the narrow band-gap, the VLWIR detectors are easily affected by a lot of factors, including the materials, fabrication technology, lab environment etc. So the ratio of dead pixels is more than 10% in Tab.1. On the other hand, Because of the carrier freeze-out effect and the increase of the threshold voltage[11], the open-loop gain of amplifier and overall voltage swing will decrease significantly at the temperature of 50 K, and the BDI′s injection efficiency will be reduced by the low impedance of the detectors. It will lead to increase the nonuniformity of the responsivity by the inconsistency of the detector′s units. Besides, the output signal is seriously impacted by the high background noise of stirling refrigerator,

and its′ RMS noise is about 0.9 mW.

In the following work, it is necessary to improve the performance of VLWIR FPA in two aspects, detectors and ROIC. Furthermore, the characteristics of FPAs will be better evaluated with a proper testing system.

3 Conclusions

The fabrication technology and performance of VLWIR detector have been introduced and presented. Furthermore, the ROIC with improved background suppression has been designed and analyzed for the VLWIR FPAs′ itself defects. According to the testing results of FPAs, the output swing is over 2 V, and the maximum readout clock frequency can reach 2.5 MHz in two models. For a 14.3 μm cutoff wavelength operating at 50 K, the peak detectivity and blackbody responsivity of PFAs can achieve to a very high level. In addition, the reason for poor dead pixels ratio and nonuniformity of responsivity has been studied, and a theoretical foundation is established for the following research.

References:

[1] Wang Yinfeng, Tang Libin. Advances in third-generation HgCdTe devices [J]. ***Electro-optic Technology Application***, 2009, 24(5): 17-22.

[2] Gravrand O, Mollard L, Largeron C, et al. Study of LWIR and VLWIR focal plane array developments: comparison between p-on-n and different n-on-p technologies on LPE HgCdTe [J]. ***Journal of Electronic Materials***, 2009, 38(8): 1733-1740.

[3] Xie Xiaohui, Liao Qingjun, Yang Yongbin, et al. Electro-optical characteristics of HgCdTe very long wavelength infrared photovoltaic detector [J]. ***Infrared and Laser Engineering***, 2013, 42(5): 1141-1145. (in Chinese)

[4] Liu Xiaolei, Yu Songlin. Design analysis of ROIC for LWIR application [J]. ***Laser & Infrared***, 2009, 39(2): 119-122. (in Chinese)

[5] Zhao Chen, Ding Ruijun. Background suppression of readout circuits for IR detectors [J]. ***Laser & Infrared***, 2007, 37(S): 981-984. (in Chinese)

[6] Hao Lichao, Ding Ruijun, Li Hui, et al. Shared readout integrated circuit with memory-function background suppression [J]. ***Infrared and Laser Engineering***, 2015, 44 (11): 3293-3298. (in Chinese)

[7] Hao Lichao, Ding Ruijun, Zhang Junling, et al. A high-performance readout circuit (ROIC) for VLWIR FPAs with novel current mode background suppression [C]//IEEE International Conference on measurement, information and control, 2012: 869-873.

[8] Zhou Yangfan, Xie Liang, Xia Xiaojuan, et al. Design of pixel readout circuit with time-sharing background suppression[J]. ***Laser & Infrared***, 2009, 39(11): 1219-1222. (in Chinese)

[9] Phillip E Alllen, Douglas R Holberg. CMOS Analog Circuit Design [M]. 2nd edition. Beijing: Publishing House of Electronics Industry, 2011: 78-80.

[10] Robert F Cannata, Randal J Hansen, Adrienne N Costello, et al. Very wide dynamic range SWIR sensors for very low background applications[C]//SPIE, 1999, 3698: 756-765.

[11] Liu Wenyong, Feng Qi, Ding Ruijun. Impact of Kink Effect on CMOS Readout Circuits for cryogenic operation[J]. ***Laser & Infrared***, 2007, 37: 990-992. (in Chinese)